Journal of Technology Research (JTR)
Volume 5, Issue 2, (2025), pp 113-119, ISSN 3005-639X

Residential Solar Collectors Investigation Using Numerical Methods

Abdulbasit S. Alkharbash [1], Mabruk M. Abugderah [2], Ali K. Muftah [2*]

[1] Mechanical Engineering Department, Faculty of Engineering, Zawia University, Zawia, Libya.

[2] Mechanical Engineering Department, Faculty of Engineering, Sabratah University, Sabratah, Libya.

*Corresponding author email: ali.muftah@sabu.edu.ly.

Received: 29-10-2025 | Accepted: 05-12-2025 | Available online: 15-12-2025 | DOI:10.26629/jtr.2025.13

ABSTRACT

A mathematical model was developed to investigate thermal performance of residential solar collectors. The effect of operational and geometrical parameters on the system thermal performance was analysed. The results have shown a good agreement compared with experimental and theoretical results obtained from the literature. The difference between the two was in the order of 2.8% and 3.5%, respectively. Results showed that the thermal performance of flat plate solar collectors are influenced with different impact degrees by insulation, wind speed, water flow rates, solar irradiance and ambient temperature.

Keywords: Heat transfer, solar collector, Numerical analysis, two dimension.

تحليل ثنائي الأبعاد لمجمع الطاقة الشمسية ذي اللوحة المسطحة

عبد الباسط الخرباش[1]، المبروك ابوقديرة[2]، علي مفتاح[2]

[1] قسم الهندسة الميكانيكية ، كلية الهندسة الزاوية ، جامعة الزاوية ، الزاوية، ليبيا.

[2] قسم الهندسة الميكانيكية ، كلية الهندسة صبراتة ، جامعة صبراتة ، صبراتة، ليبيا.

ملخـــــــص البحــــــث

يُعَدّ التحليل العددي أداة فعّالة توفر الوقت والجهد وتقلل من التكلفة مقارنة بالطرق العملية التي غالبًا ما تكون باهظة الثمن وتستغرق وقتًا طويلاً. في هذه الدراسة، تم إجراء تحليل حراري ثنائي الأبعاد بهدف تطوير نموذج رياضي يُمثّل الاتزان الحراري للمجمعات الشمسية، وذلك للحصول على منهج نظري لتصميم المجمعات الشمسية المسطحة.

تمت دراسة الخصائص التصميمية وتأثير العوامل التشغيلية والهندسية على أداء المجمع. كما تمت مقارنة النتائج مع بيانات عملية تم الحصول عليها من نماذج اختبارية حقيقية، وأظهرت النتائج توافقًا جيدًا مع البيانات التجريبية، حيث لم تتجاوز نسبة الخطأ **2.8%** مقارنة بالنتائج العملية. كذلك تمت مقارنة النتائج مع بيانات التحليل الحراري أحادي البعد للمجمعات الشمسية المسطحة، وبلغت نسبة الخطأ حوالي **3.5%.** وأظهرت النتائج أيضًا أن كلًّا من العزل الحراري للمجمع وسرعة الرياح لهما تأثير سلبي على الكفاءة الحرارية للمجمع الشمسي، بينما معدل تدفق الماء والإشعاع الشمسي ودرجة الحرارة المحيطة تؤثر إيجابيًا على الكفاءة الحرارية بدرجات متفاوتة من التأثير.

الكلمات الدالة: انتقال الحرارة، المجمع الشمسي، التحليل العددي، ثنائي الأبعاد.

1. INTRODUCTION

The increasing global demand for renewable energy has led to extensive research on solar energy systems as clean and sustainable alternatives to fossil fuels. Among these systems, flat-plate solar collectors (FPCs) are the most common and reliable devices for low-temperature applications such as water heating, solar desalination, and process heat.

The performance of a flat-plate solar collector depends on several factors, including solar irradiance, ambient temperature, wind speed, and collector design. Although experimental evaluation provides accurate results, it is often costly and time-consuming. Therefore, numerical modelling offers an efficient alternative for predicting thermal performance and optimizing design parameters.

Conventional one-dimensional analyses simplify the problem but may not capture the real temperature gradients over the absorber plate. In contrast, two-dimensional modelling provides a more accurate representation of heat transfer and temperature distribution within the collector. This study presents a 2-D numerical analysis of a flat-plate solar collector to evaluate the influence of different operational and geometrical parameters on its thermal efficiency.

.H. Kazeminejad studied a temperature distribution over the absorber plate of a parallel flow, flat-plate solar collector is analyzed with one- and two-dimensional steady-state conduction equations with heat generations using a control volume-based finite difference scheme [1]. They found out that one-dimensional analysis slightly deviates from two-dimensional analysis, particularly under low mass flow rate conditions. S.Farahat et al presented an exergetic optimization of flat plate solar collectors to determine the optimal performance and design parameters [2]. The developed computational program was in good agreement with the experimental measurements noted in the previous literature. Finally, the exergetic optimization has been carried out under given design and operating conditions and the optimum values of the mass flow rate, the absorber plate area and the maximum exergy efficiency have been presented.

The description of solar heating systems can be found in Duffie and Beckman [3]. They normally consist of a solar collector and a working fluid storage tank connected with pipes. Depending on the application objective, the water is pumped or naturally flows from the collector to the tank and back to the collector through the pipes.

2. MATHEMATICAL MODELLING

The input properties and calculation parameters used for the three collectors in this study are summarized in Table 1.

Governing equations are obtained from the energy balance on the absorbing plate, Kirchhoff and Billups [3]:

$$k_f \delta_f \left(\frac{\partial^2 T_f}{\partial x^2} + \frac{\partial^2 T_f}{\partial y^2}\right) + (\tau\alpha)_e H_t = h_{fg}\left(T_f - T_g\right) + \left(\frac{\sigma}{\varepsilon_g^{-1} + \varepsilon_f^{-1} - 1}\right)\left(T_f^4 - T_g^4\right) \qquad (1)$$

Boundary conditions:

$$\left.\frac{\partial T_f}{\partial y}\right|_{(x,0)} = \left.\frac{\partial T_f}{\partial y}\right|_{(x,l)} = 0 \quad \text{and} \quad \left.\frac{\partial T_f}{\partial x}\right|_{(0,y)} = \left.\frac{\partial T_f}{\partial x}\right|_{(w,y)} = 0$$

The relation between the working fluid and the tube surface is given by:

$$\frac{\partial T_w}{\partial y} = \frac{h_{rw}\pi D_r}{\dot{m} C_p}\left(T_f\Big|_{x=w/2} - T_w\right) \qquad (2)$$

The governing equation of the glass cover is obtained from the energy balance, Hobson and Norton [3]:

$$k_f \delta_f \left(\frac{\partial^2 T_f}{\partial x^2} + \frac{\partial^2 T_f}{\partial y^2}\right) + (\tau\alpha)_e H_t = h_{fg}(T_f - T_g) + U_{fa}(T_f - T_a) + \left(\frac{\sigma}{\varepsilon_g^{-1} + \varepsilon_f^{-1} - 1}\right)(T_f^4 - T_g^4) \quad (3)$$

In this study the fin and pipe are considered as one part which means that the governing equation of the heat transfer in the collector absorbing plate and working fluid are treated separately: Figure (1) shows the heat transfer mechanism from the fin to the tube and from the tube to the working fluid.

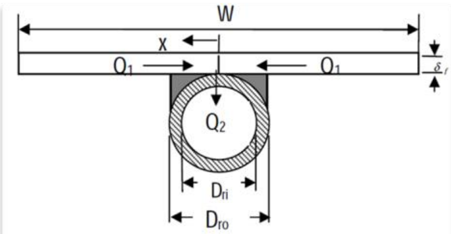

Fig1. Fin and tube section.

From the previous figure we obtain the following expression:

$$2Q_1 = Q_2 \quad (4)$$

where Q_1 and Q_2 are the energy transfer from the fin and the energy transfer from the fin surface to the working fluid respectively and therefore:

$$2\left(-k_f \delta_f \left.\frac{\partial T_f}{\partial x}\right|_{(0,y)}\right) = U_{fw} \pi D_{ri} \left(T_f|_{x=0} - T_w\right) \quad (5)$$

The two dimensional fin energy equation is,

$$k_f \delta_f \left(\frac{\partial^2 T_f}{\partial x^2} + \frac{\partial^2 T_f}{\partial y^2}\right) + (\tau\alpha)_e H_t = h_{fg}(T_f - T_g) + U_{fa}(T_f - T_a) + \left(\frac{\sigma}{\varepsilon_g^{-1} + \varepsilon_f^{-1} - 1}\right)(T_f^4 - T_g^4) \quad (6)$$

The boundary conditions are,

$$\left.\frac{\partial T_f}{\partial x}\right|_{(w/2,y)} = 0 \quad \left.\frac{\partial T_f}{\partial y}\right|_{(x,0)} = \left.\frac{\partial T_f}{\partial y}\right|_{(x,l)} = 0$$

and $\left.\frac{\partial T_f}{\partial x}\right|_{(0,y)} = \frac{-U_{fw} \pi D_{ri}}{2 k_f \delta_f}\left(T_f|_{x=0} - T_w\right)$

where U_{fw} is the heat transfer coefficient between the working fluid and tube. The governing equation of the working fluid in the tube is given by:

$$\dot{m} C_w \frac{\partial T_w}{\partial y} = h_{rw} \pi D_{ri} (T_s - T_w) \quad (7)$$

where h_{rw} and T_S are heat transfer coefficient between the working fluid and tube internal surface and internal tube wall surface temperature respectively.

Boundary conditions:

$$T_w|_{y=0} = T_{in}$$

The glass cover energy balance equation is given by:

$$h_{gf}(\overline{T}_f - T_g) + \left(\frac{\sigma}{\varepsilon_g^{-1} + \varepsilon_f^{-1} - 1}\right)\left(\overline{T}_f^{\,4} - T_g^4\right) = h_{wind}(T_g - T_a) + \sigma \varepsilon_g (T_g^4 - T_{sky}^4) \quad (8)$$

The governing equation together with their boundary conditions were solved by finite difference method using MATLAB software. The instantaneous efficiency based on the total collector area is calculated by:

$$\eta_c = \frac{Q_u}{A_c G} \quad (9)$$

3. RESULTS AND DISCUSSION

The algorithms in the study were optimized through the number of nodes used in the grid. Figure (2) shows the error obtained in the exit working fluid temperature in function of the number of nodes in the X-direction. As it can be verified, the error is inversely proportional to the number of nodes. After the 45 nodes the change in the error can be considered as negligible and therefore, this number was considered to be the optimum. The number of nodes in the Y direction was not given attention because it has no influence on the results due to the fact of insignificant change in temperature distribution in this direction.

Table 1. Input properties and calculation parameters.

Property/ Condition		1st collecter [4]	2nd collecter [5]	3rd collecter [6]
$F_R\tau\alpha$		0.786	0.808	0.766
F_RU_l		4.357	4.668	4.592
Solar Intensity (W/m^2)		854	850*	800*
Wind Speed (m/s)		3	3*	4*
Water flow rate (kg/h)		145	200*	190*
Inclination Angle (degrees)		45	45	45
Collector area (m)		2.272	2.024	2.49
Port area (m)		2.013	1.825	2.259
Absorbing Surface area (m)		2.018	1.782	2.26
Collectors dimensions (m)	Length (m)	2.090	2.008	2.008
	Width (m)	1.087	1.008	1.24
	Thickness (m)	0.105	.086	0.102
Absorbing Surface				
Material		Copper	Aluminium	Copper
Absorbance		95%	97%	95%
Emissivity		5%	5%	5%
Thickness (mm)		0.2	0.5	0.2
Tube				
Material		Copper	Copper	Copper
Tubes Number		8	8	10
Internal Diameter (mm)		6.4	9.2	7
External Diameter (mm)		8	10	8
Cover				
Material		Glass	Glass	Glass
Transmittance		90.6%	90%*	90.5%
Thickness		4	4	4
Insulation				
Type of Insulation		Mineral wool	Glass wool	Glass wool
Back Ins Thickness (mm)		66	30	50
Edge Thickness (mm)		20	15	20
Thermal conductivity (W/m.K)		0.045	0.035*	0.046*

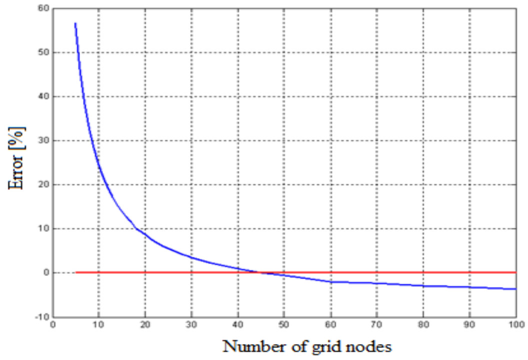

Fig 2. Algorithms error in function of mesh grid.

The same conclusion can be obtained from Figure (3), which presents the relationship between the outlet temperature and the mesh grid. The outlet temperature reaches almost steady state when the grid in the X-direction reaches 45 nodes.

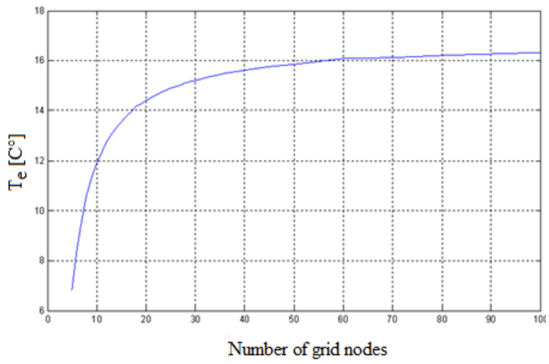

Fig 3. The influence of the grid on the outlet temperature.

After specifying the optimum grid size, the program was tested using flat plate solar collector results obtained by international solar energy centres according to European Standards (EN12975) Table 1. Three different reports were used. Figure (4) shows the flat plate solar collector in function of (Tm-Ta) for the one- and two-dimensional solutions compared to the first tested collector results. As it can be seen, the results obtained by the developed algorithms have the same trend of those obtained experimentally.

$$\eta_c = F_R\tau\alpha - F_RU_l\left(\frac{T_{in}-T_a}{G}\right) \quad (10)$$

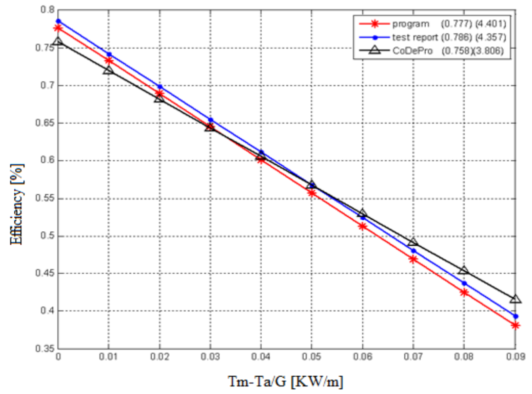

Fig4. Comparison between one and two dimensional algorithm results and the tested collector.

$$\eta_{1Program} = 0.777 - 4.401\left(\frac{T_{in} - T_a}{G}\right) \quad (11)$$

$$\eta_{1CoDePro} = 0.758 - 3.806\left(\frac{T_{in} - T_a}{G}\right) \quad (12)$$

Thermal conductivity of any material is directly proportional to temperature. Normally the average value of the insulation material is taken. This value is inaccurate in obtaining good results using the program. Figure (5) shows the relationship between the thermal efficiency of the solar collector and the insulation material thermal conductivity. As it can be noted, the solar collector thermal efficiency decreases steadily with the increase in insulation thermal conductivity and ends at an efficiency of about 0.69 at an insulation of 0.095. This decrease in the efficiency is due to the increase in the heat loss with the increase with the thermal insulation. The thermal resistance of contact between the pipes and the absorbent plate is usually not considered, but in some design cases it could be very high. In this study, it is considered to be sufficiently high to be neglected.

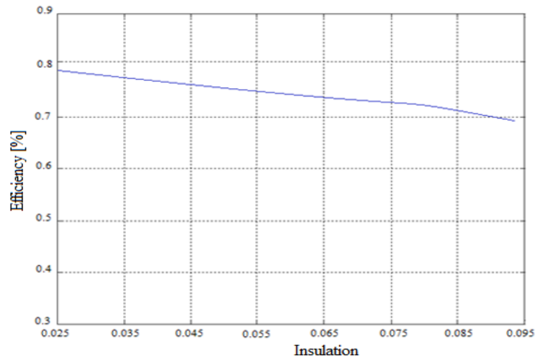

Fig 5. Effect of insulation on the solar collector thermal efficiency.

The rate of water flow within the solar collector contributes significantly to the process of transferring heat from the solar collector to the water tank. Since increasing the flow rate would lead to an increase in the amount of heat obtained from the solar collector, which would consequently increase the efficiency of the solar collector. However, this is not always true, especially when the solar collector is connected to the thermal reservoir in open circuits. In some cases increasing the working fluid flow rate could increase the heat transfer loss and therefore, it will negatively affect the temperature of the water inside the reservoir. To obtain the optimal flow rate, there is a strong need to conduct further research. In most cases, the flow rate should be close to the value of $0.02\frac{kg}{m^2 s}$ unless the solar collectors manufacturers specify otherwise. Figure (6) shows the relationship between the thermal efficiency and the flow rate. The thermal efficiency is directly proportional to the flow rate.

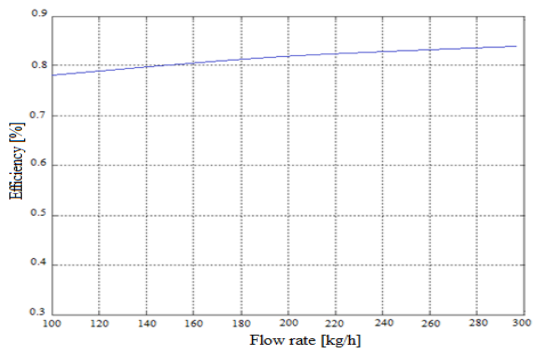

Fig 6. Effect of water flow rate on the solar collector thermal efficiency.

Wind is one of the most important factors affecting the heat loss coefficient in the solar collector. The specification determined that the wind speed in the tests is between 2 to 4 $\frac{m}{s}$. Figure (7) shows the effect of wind speed on the thermal efficiency of the solar collector. In fact, the change could be even greater. Here, the mathematical model and heat transfer equations used in the program are insufficiently accurate and makes a disadvantage of the program. The effect is small for a wind speed up to 25 $\frac{m}{s}$. The thermal efficiency is inversely proportional the wind speed. The enhancement of heat losses due to wind speed increase contributes to an efficiency decrease.

Figure (8) shows the influence of atmospheric air temperature on the solar collector's efficiency curve. It is observed that the thermal efficiency increases with the increase of the atmospheric temperature and that would be due to the heat losses to the environment caused by temperature gradient increase.

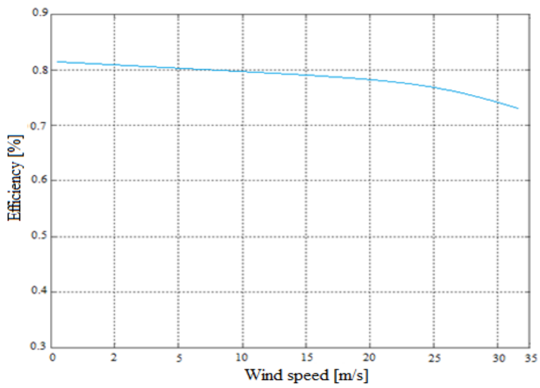

Fig 7. Influence of wind speed on the solar collector thermal performance.

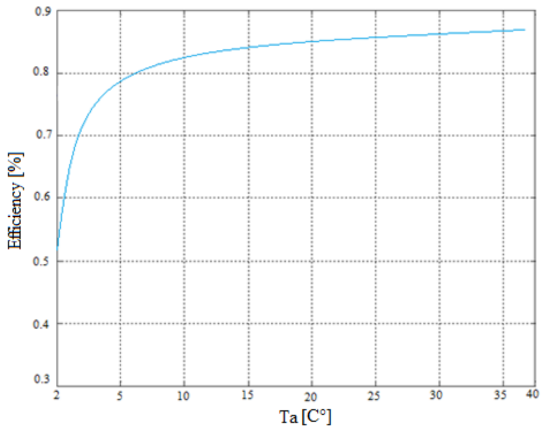

Fig 8. Effect of ambient temperature on the collector thermal efficiency

4. THEORY AND CALCULATION

The theory should extend, not repeat, the background to the article already dealt with in the introduction and lay the foundation for further work. In contrast, calculations represent a p

Testing standards did not specify a fixed value for the intensity of solar radiation. The American Standard (ASHRAE) in this regard stipulates that the value of solar radiation should not be less than (790 W/m^2) and should not change during the test by more than (± 32 W/m^2). On the other hand, ISO 9806-1 specifies test radiation intensity to be $800W/m^2$and the radiation variation to be not more than 50 W/m^2. It also states that the ratio of diffuse radiation to total radiation should not exceed 20%. Figure (9) illustrates the effect of solar radiation intensity on the determination of the solar collector's efficiency curve. Note that the solar radiation intensity has a significant effect on the performance of the solar collector. The efficiency goes from 0.3 for radiation intensity of 100 to about 0.78 for solar radiation intensity of 1300 W. The variation in solar radiation intensity can occur in the nature due to climate change such as clouds, fog or dust.

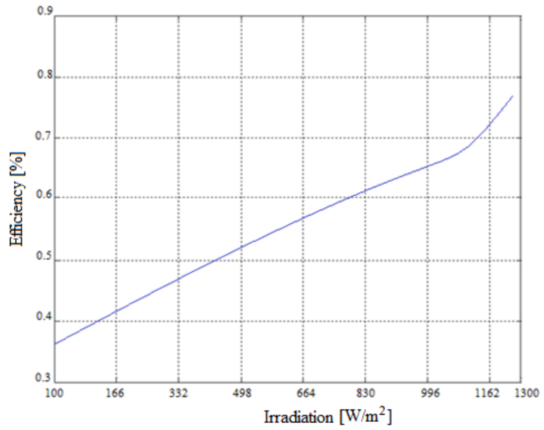

Fig 9. The influence of irradiation on the collector thermal efficiency.

5. CONCLUSIONS

In this study a two dimensional model of a solar collector was modelled, coded and solved in order to determine the effect of the operational parameters on the thermal performance of the solar collector. The developed program is a reliable tool to design and evaluate flat plate solar collectors. The contact resistance of the welding between the tubes and the absorbing plate has negligible effect on the performance of the solar collector. On the other hand, the flow rate of the working fluid and the wind velocity have had moderate influence on the efficiency of the solar collector. The solar irradiance has a significant effect on solar collector's thermal performance. It is recommended that future work include provisional modeling and additional local pilot testing to further refine the numerical model.

REFERENCES

[1]. H.Kazeminejad 'Numerical analysis of two dimensional parallel flow flat-plate solar collector' Renewable Energy, Volume 26, Issue 2, June 2002, Pages 309-323.

[2]. S. Farahat, F.Sarhaddi and H. Ajam, Exergetic optimization of flat plate solar collectors, Renewable Energy, Volume 34, Issue 4, April 2009, Pages 1169-1174.

[3]. Hobson and Norton [3]

[4]. Kirchhoff and Billups

[5]. Duffie, J.A., and Beckman, W.A., 1996, Solar Engineering of Thermal Processes. edition, John Wiley & Sons, Inc., New Jersey.

[6]. Test Report: KTB Nr. 2004-05, Collector test according to EN 12975-1,2, Fraunhofer institute

[7]. Test Report: KTB Nr. 2008-k2-en, Efficiency test according to EN 12975-2:2006, Fraunhofer institute

[8]. F.M. White, Fluid Mechanics, 7th Edition, McGraw-Hill, New York, 2009, ISBN 978–0–07–352934–9